Available online at www.sciencedirect.com
SCIENCE DIRECT®

Journal of the European Ceramic Society 23 (2003) 3125–3134
www.elsevier.com/locate/jeurceramsoc

Long term oxidation of a SiC fiber-bonded composite in air at 1500 °C

Akihiko Otsuka*, Yoshikazu Matsumura, Kazuya Hosono, Ryohei Tanaka

Japan Ultra-high Temperature Materials Research Institute (JUTEMI), Okiube 573-3, Ube-city, Yamaguchi 755-0001, Japan

Received 5 December 2002; received in revised form 13 February 2003; accepted 22 February 2003

Abstract

The oxidation behavior of the SiC fiber-bonded composite (Tyrannohex^{TM}) was investigated at 1500 °C up to 4000 h in air. During heating of the samples, it was observed that an amorphous SiO_2 scale was formed and that bubbles of SiO_2 were generated due to the gaseous products upon oxidation. A large mass loss was also observed after 4000 h heating in spite of the condition of passive oxidation for SiC. The cause of large mass loss can be explained by destruction of oxidation protective scale due to bursting of the bubbles, and high oxidation rate due to high oxygen mobility in amorphous SiO_2 scale containing aluminum ions. To prevent this accelerated oxidation of the composite, a double-layered coating using a CVD-SiC process was developed. Although the samples coated with CVD-SiC were stable in this oxidation test, the cristobalite peaks observed by XRD suggest also an inherent problem of the SiO_2 scale spalling.

Keywords: Coatings; Composites; Cristobalite; CVD coating; Interfaces; Oxidation; SiC/SiC

1. Introduction

Ceramic matrix composites (CMCs) or continuous fiber ceramic composite (CFCC) with high fracture toughness as compared to monolithic ceramics have been developed for their high performances at high temperatures in air. In order to keep their mechanical properties, the ceramic fibers must be very stable under reactive and particularly oxidative atmospheres during the processing and the practical using of the composites. Different types of fiber material compete for those applications. However, the constituent fiber for CMCs used at high temperatures is presently limited in non-oxide fibers such as SiC or SiCBN because of their good creep resistance property at high temperatures.

Then, CMCs with SiC fiber are expected to be used at high temperatures. The fibers used in them are one of the typical applications of the polymer-derived ceramics, invented by Yajima et al. in the 1970s.[1] They are produced by conversion of a polymer precursor to a mixture of amorphous and nanocrystalline phases of SiC.[2,3] However, during the first stage of their development, they had a limited temperature range for high temperature applications due to the insufficient stability of microstructure. One of the ways to extend the range to higher temperatures is to decrease the oxygen content, second phases, and to increase grain size of the crystallites in the SiC fibers.[4–6] Now, the increasing attention to the metal-containing polymer precursors is also providing new potential for nano-structured composites. These polymers are basically homogeneous and can be converted to an ultra-fine ceramic structure that is stable at very high temperatures. The active metal in polymer works as an acceptor of residual oxygen and improves sintering activity.

The most stable SiC fibers known so far are those developed by Ishikawa et al.[7] Although, ordinary SiC fibers had been fabricated by sintering a polymer precursor at 1300 °C. The newly developed SiC fibers are produced by sintering at 1900 °C an amorphous Si–Al–C–O precursor fabricated by the melt-spun of polyaluminocarbosilane at low temperatures. On the contrary, the produced fibers are composed of nearly stoichiometric SiC that is considered the main reason for the microstructural stability. They have clearly shown full strength retention up to 1900 °C and 80% retention of the initial room temperature strength after heat-treatment at 2000 °C for 1 h in argon. The creep

* Corresponding author.
E-mail address: akihiko@c-able.ne.jp (A. Otsuka).

0955-2219/03/$ - see front matter © 2003 Elsevier Ltd. All rights reserved.
doi:10.1016/S0955-2219(03)00116-X

resistance of the fibers at 1300 °C is significantly higher than that of ordinary SiC fibers.

Another important issue of the CMCs is an interface between the fibers and matrices. Since the interface strength in CMCs determines their crack resistance, a special interface or inter-phase is normally introduced into the composite structure. CMCs usually have either carbon or boron nitride interphase which is acting as a weak interface. An example of creating a favorable interface by self-assembling has been also given by Ishikawa et al.[8] Cross plies of amorphous Si–Al–C–O woven fibers obtained from a polyalminocarbosilane precursor were stacked together to form a two-dimensional sheet, which was hot-pressed at a temperature of 1900 °C under 50 MPa of Ar. The process resulted in a thin carbon layer between the fibers and conversion of the amorphous fiber into β- and/or α-SiC fibers of hexagonal cross-section, which is so-called prismatic structure. The carbon layer acts as an interphase yielding a fracture mechanism with much fiber pull-out and favorably high fracture energy, of about 2000 J m^{-2}.

The problem of microstructural stability of CMCs arises inevitably when they are used at high temperatures in oxidizing atmospheres. The carbon interphase provides the appropriate strength as described above, but it reacts easily with oxygen to form either carbon monoxide or carbon dioxide at temperatures as low as about 500 °C. Boron nitride readily forms a low-viscosity B_2O_3 liquid phase at temperatures less than 1000 °C that leads to high mobility of various species that can affect the microstructure of other components.[9] Therefore, both oxidation kinetics and mechanical properties of the composites have been studied thoroughly.[10–13] After complete removal of carbon as carbon monoxide or carbon dioxide, oxygen reacts with the SiC fiber to form a SiO_2 layer, which leads both to weakening of the fiber and to strengthening of the fiber–matrix interface resulting in a drastic decrease in fracture toughness of the composite. One of the possible solutions for prevention of oxidation of carbon and boron nitride at an interface, therefore, should be oxidation protective coating on the surface of the composites.

In this paper we report recent results on the stability of SiC fiber-bonded composite derived from an aluminum-containing polymer at 1500 °C for long term in air. In addition, a new concept for oxidation protective coating by a double-layered SiC coating is also demonstrated.

2. Experimental procedure

2.1. SiC fiber-bonded composite

The SiC fiber-bonded composite tested in this work was Tyrannohex™ that was fabricated by Ube Industries Ltd., and consisted of cross-ply (0°/90°) of the Tyranno™ fibers (Si–C–Al–O). This composite was developed by Ishikawa et al.[8] as mentioned earlier, and the carbon interphase was deposited from the fibers during hot pressing at 1900 °C in Ar. Using transmission electron microscopy (TEM), the carbon interphase of this as obtained composite has been measured to be approximately 10 nm in thickness. The XRD pattern indicated the composition to be predominantly β-SiC (mixed with some amount of α-SiC), cristobalite and a very small amount of graphite phases. It is recalled that the aluminum organic compound, oxygen and excess carbon contained in the amorphous Si–C–Al–O fibers are vaporized as aluminum carbide and silicon monoxide during the hot pressing at 1900 °C.

The dimensions of the polished substrate after cutting from the bulk were 3×4×40 mm, and all of the faces of the sample had been previously oxidized (with formation of a layer of cristobalite as supported by XRD) under certain oxygen partial pressure for inhibition of the oxidation of the in-depth carbon interphase. The sample showed dark purple red color due to the SiO_2 protective scale of about 50 μm thick.

2.2. A double-layered SiC coating on the specimen

This coating process was originally developed for improvement in oxidation resistance of a C/C composite by the authors and the detail of the procedure has been described elsewhere..[14,15] The surface of the previously oxidized substrate was firstly coated with Si powder + polyvinylalcohol (PVA) slurry and heated at 1500 °C for 2 h in Ar in order to remove the SiO_2 overlayer that had already been made by oxidizing. SiC conversion from the carbon interphase deposited between the fibers near the surface of this composite has also occurred at the same time. The adhesive strength of the upper coating layer formed by the following process described below, can be improved by this surface treatment.

Fig. 1 shows the fabrication process of the double-layered SiC coating. The surface-pretreated substrate by Si powder was coated again with the slurry containing finely dispersed powdered carbon fiber, Si powder and polycarbosilane (xylene solution). These constituents (Si powder and powdered carbon fiber) were selected to form a SiC/SiC composite layer through the following CVD process. This composition limited to carbon and silicon, was made not to lower the melting point of SiO_2-scale formed by high temperature oxidation. It is very important not to increase the oxygen permeability of the SiO_2-scale. The powdered carbon fiber is a commercially available milled fiber material (Toho Tenax Co., Ltd., HTA-CMF-0040-E), about 40 μm in average length. The binder of the slurry was 17.8 mass% polycarbosilane (PCS, Nippon Carbon Co., Ltd.) in xylene. The composition of the slurry shown in Table 1 is an example for synthesis of the Si-rich SiC layer.

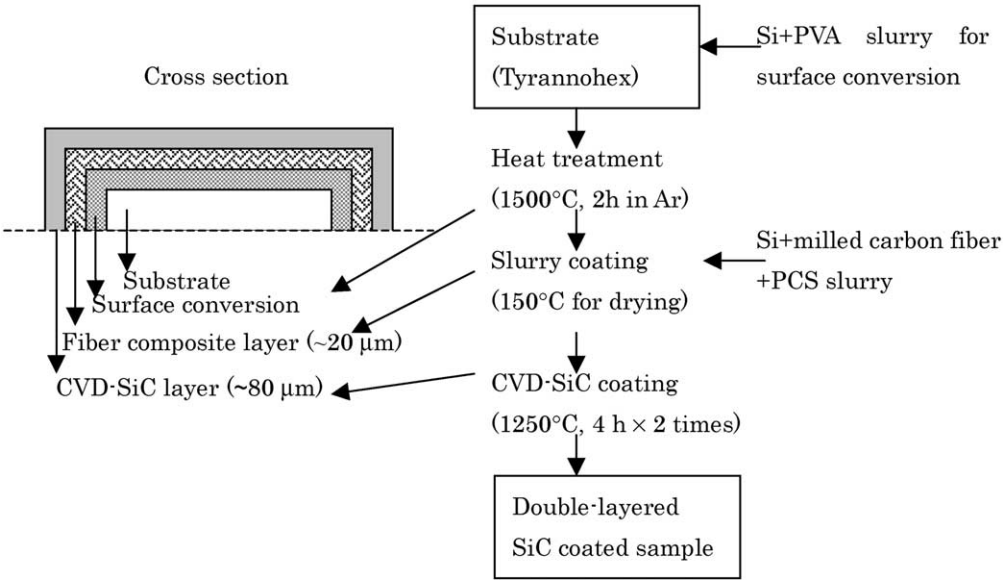

Fig. 1. Schematic diagram for double-layered SiC coating process.

Table 1
Composition of the slurry for coating

Material		Mass ratio (%)
Powdered carbon fiber (milled fiber)	HTA-CMF-0040-E, Toho Tenax Co., Ltd. Average fiver length: 40 μm	8.6
Si powder	Kojundo Chemical Lab. Co., Ltd. Purity: 99.999%, 300 mesh under	20.0
Polycarbosilane (PCS)	Nipsi Type S, Nippon Carbon Co., Ltd.	17.8
Xylene	Wako Pure Chemical Industries, Ltd.	53.6

With respect to this fiber composite layer, it should be emphasized here, a Si-rich matrix is generally more stable, in terms of oxidation resistance, at high temperatures than a C-rich matrix, because of less formation of CO and/or CO_2 gaseous species. It is easy to control its composition by changing the ratio of powdered carbon fiber and Si powder contents. The coated sample was dried at 150 °C in air and then densified through the following CVD-SiC process. The thickness of the coated layer was about 20 μm.

CVD-SiC was formed at 1250 °C, under a total gas pressure of 1.3 kPa, at gas flow rates of 8.3×10^{-6} m^3 s^{-1} for $SiCl_4$ and CH_4, and 50×10^{-6} m^3 s^{-1} for H_2 gas, respectively. After coating for 4 h, the coated samples were turned over and coated for 4 h again in the same way to make a uniform thickness of the resulting coating. A double-layered SiC coating of about 100 μm in total thickness could be obtained under these conditions. When SiC is deposited inside the pore of the fiber composite coating layer during the CVD processes, ceramization of PCS to SiC and reaction sintering of powdered carbon fiber and Si powder also occurred at the same time.

2.3. Oxidation test

Oxidation resistance of the samples was examined at 1500 °C at certain time intervals up to 4000 h in a constant airflow at a pressure of about 0.1 MPa. Fig. 2 shows a schematic diagram of the oxidation testing apparatus. The flow rate of dry air was 3.3×10^{-6} m^3 s^{-1}. The SiC fiber-bonded composite samples were mounted on a sample holder (made from SiC, which purity is approx. 97.5% and it contained approx. 0.35% of a free carbon, the other impurities being Fe, Si and SiO_2) in a vertical position and manually loaded into a high purity Al_2O_3 box furnace for the desired oxidation time. The heating rate was 750 °C h^{-1}. Air was passed through a molecular sieve (silicagel) in order to dry it. After a certain heating time interval, some of the samples were taken out from the furnace, and their mass changes were measured.

In order to reduce the influence of the sodium contamination from the wall of the furnace, the high purity Al_2O_3 box furnace had been preheated at 1500 °C for 50 h passing air before use for the oxidation tests. However, the sodium contamination is caused from anywhere such as the passing air, therefore, it is difficult to prevent. Therefore, oxidation behavior has been investigated by comparing the stability of the samples with pure SiC (CVD-SiC).

The residual strength was also measured by using four-point flexural test with a floating self-aligning fixture with an inner span of 10.00 mm and an outer span

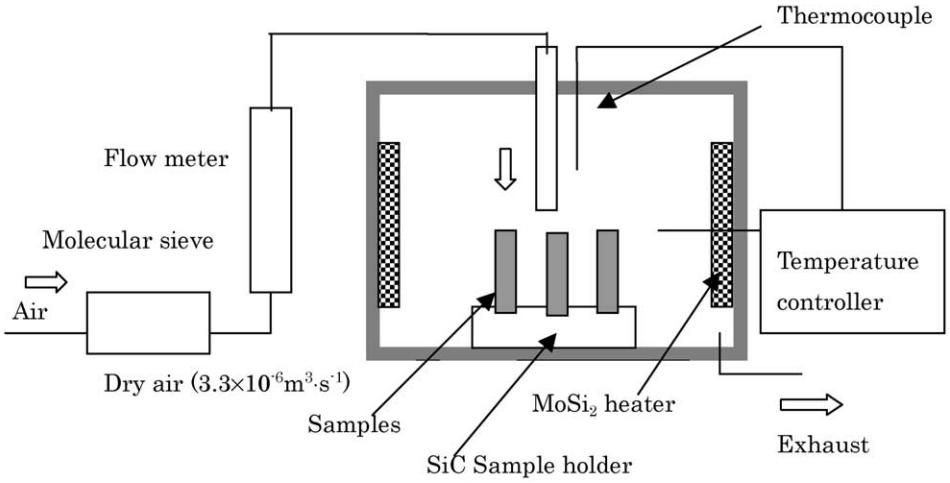

Fig. 2. Schematic diagram of the oxidation apparatus used in the test.

of 30.00 mm. Cross head speed was 0.5 mm/min. Three to six samples were tested at each condition. The remaining samples were heated again up to the desired time (intervals), therefore, the samples heated for long time intervals had the more cyclic heat history.

3. Results and discussion

3.1. Oxidation of the composites

Typical kinetic curves of oxidation are shown in Fig. 3 for samples without coating (a) and with coating (b). The mass changes in both of the samples measured for the first 500 h of oxidation showed parabolic feature due to the SiO_2 scale growth. However, after 500 h heating the mass of the sample without coating tended to decrease with an increment of the heating time, and finally large mass loss was observed after 4000 h heating showing localized heavy degradation. The surface of the sample changed its color to white from original dark purple-red color. During the heating of the samples, it was also observed that a glassy SiO_2 scale was formed on the sample without coating and bubbles of "silica" were generated due to the gaseous oxidation product (presumably CO, and/or CO_2). On the other hand, the samples with coating showed quite less bubble formation.

In order to make clear the mechanism of bubble formation for this composite, the standard deviation of the measured size change was investigated. The results of standard deviation of the measured size and mass changes of the samples without coating after oxidation indicate that the bubble formation at the surfaces of the sample perpendicular to the laminate (out-of-plane) is much more frequent than that at the surfaces parallel to the laminate (in-plane) as shown in Fig. 4. Therefore, the cause of bubble formation at the early stage of the

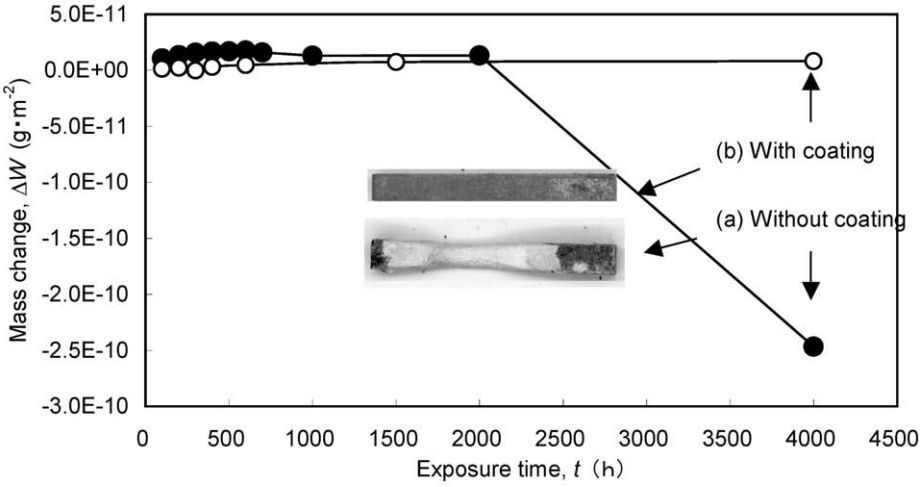

Fig. 3. Mass change, (ΔW; normalized with surface area), plotted as a function of oxidation time for SiC fiber composite samples, (a) without double-layered SiC coating and (b) with double-layered SiC coating. The samples were isothermally oxidized at 1500 °C in dry air.

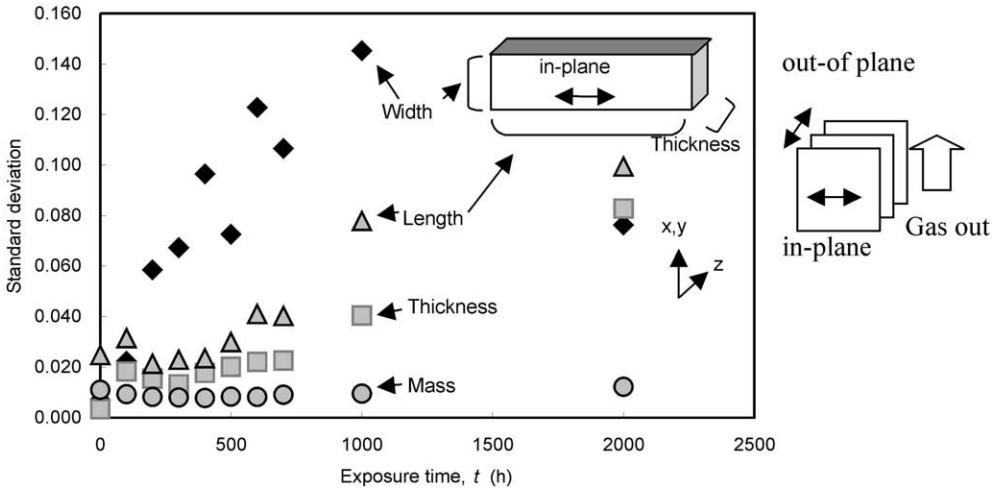

Fig. 4. Results of the calculated standard deviation of the measured data (size and mass) of the samples without coating after oxidation. Large standard deviation of the measured width of the samples indicates frequent bubble formation at the cross section of this material during heating.

oxidation of the samples without coating is considered to be mainly due to the oxidation of the carbon interphase. The frequent bubble formation in the out-of-plane direction is due to the macrostructure of the cloth ply of this composite forming a path for gaseous oxidation products.

3.2. Fracture behavior of fiber-bonded composites by four-point flexural test

Prior to the measurement of the residual strength of SiC fiber-bonded composites after oxidation, the fracture behavior of these samples before oxidation in the four-point flexural test was examined. Fig. 5(a) shows the fracture behavior observed with the samples loaded in the z direction (out-of-plane). The displacement, x, of cross head increases linearly with an increment of the applied load, P, up to 0.3 kN, indicating elastic deformation. Above the loading of 0.3 kN, the displacement increases as the result of the generation of initial crack. The maximum loads are varying from 0.33 to 0.37 kN, however, it is clear that this fiber-bonded composite has the good resistance to crack propagation as shown by the typical SEM image [inserted in Fig. 5(a)] of the crack. Interfacial failure is predominant in this sample, allowing the crack to be arrested and deflected within the carbon/SiC-fiber interface. The propagation of crack is accelerated by the increment of crack opening displacement, and it is observed that about 70% of the initial strength is lost by the initial crack. The variation of the measured fracture loads (0.33–0.37 kN) is rather small, therefore, one of the important features of stable fracture of CMCs has been demonstrated in Fig. 5(a).

Another important feature of CMCs is the possibility to control the mechanical property by changing the fiber direction of the composite. In other words, CMCs normally have anisotropic properties. Fig. 5(b) shows the fracture behavior observed with the sample loaded along the y-direction (in-plane). By changing the load direction from z to y, the fracture load increases by 60% (0.52 kN), while the fracture behavior is changed to the brittle fracture. The displacement increases linearly up to the maximum load, and the fracture occurs with rapid crack propagation. Therefore, it is clear that the fracture resistance of this composite is increased at the expense of the fracture strength.

3.3. Residual strength after oxidation

Figs. 6 and 7 show the influence of oxidation on the residual flexural strength of the samples (out-of-plane) measured by four-point flexural test, and the fracture behavior of the samples after oxidation, respectively. It should be noted in Fig. 6 that because the sample without coating after 4000 h at 1500 °C has been too much oxidized, the measurement was therefore carried out with the samples oxidized up to 2000 h. In addition, the flexural strength of samples with coating was calculated with ignoring the coating thickness because the strength of the coating is rather low. Therefore, the values of the measured flexural strength of the coated samples are comparably a little higher than that of uncoated ones.

The measured residual flexural strength of the sample without coating decreases slightly with an increment of oxidation time up to 2000 h. On the other hand, the fracture behavior was almost the same as that of the sample before oxidation, showing the deflecting crack caused by the weak interphase structure. Since, the fibers in this composite have been laminated as two-dimensional cloth ply, the fracture behavior of the sample (out-of-plane) shows a fracture similar to that of usual layered composite materials. On the contrary to this, the residual strength of the sample with coating preserves the initial strength even after oxidation for 4000 h as shown in Fig. 6, and it showed graceful failure.

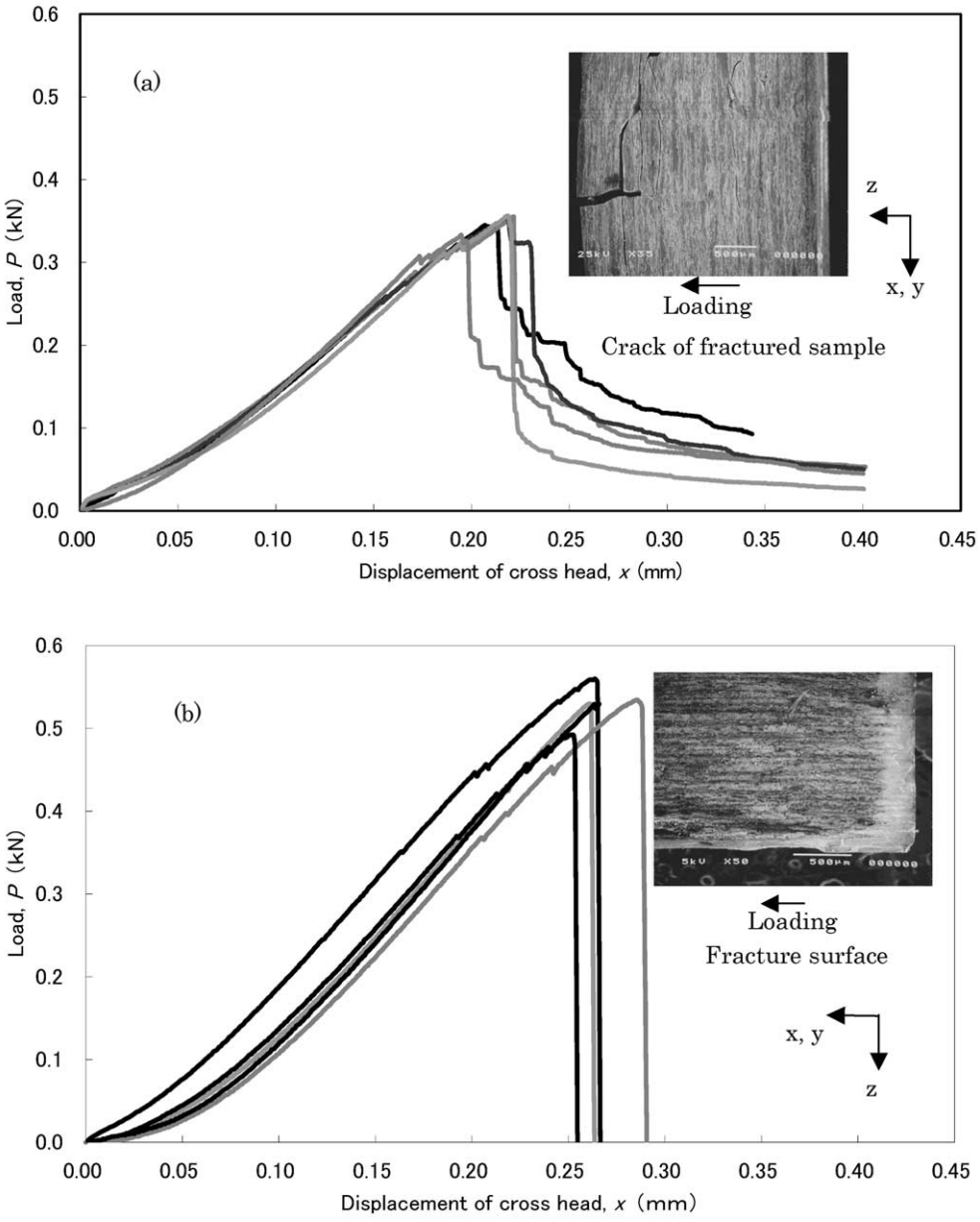

Fig. 5. Comparison of fracture behaviors of the fiber composite sample (a) loaded in the z direction (out-of-plane), (b) loaded in the y direction (in-plane). x, y and z indicate the three-dimensional direction along with the sample configuration. Different curves show the dispersion of the measured value by four-point flexural test.

Fig. 8 shows the Weibull plots of the flexural strength distribution of the samples before and after 2000 h oxidation. The strength distribution of the oxidized sample loaded along the y-direction (out-of-plane) is wide with a Weibull slope estimated to be 5.6, while those of the samples before oxidation are 28.5 (in-plane) and 15.3 (out-of-plane), respectively. Therefore, this SiC fiber-bonded composite displays not only a reduced fracture strength but also a lower reliability after high temperature oxidation. The reduction of the fracture strength by oxidation is considered to be due to the easy cracking of the silica scale on the surface of the samples. However, the detailed mechanism of this strength reduction has not yet been clarified. Anyway, if we assume the need for oxidation protective coating for this SiC fiber-bonded composite, this result suggests that the fracture property of the coating material affects the strength of these composites. Therefore, we should pay much attention for the selection of a coating material.

3.4. Mechanisms for accelerated oxidation of the fiber-bonded composite materials

Fig. 9(a,b) shows a comparison of the XRD profiles of the surface after 4000 h oxidation for the samples without coating (a) and with coating (b). It is observed

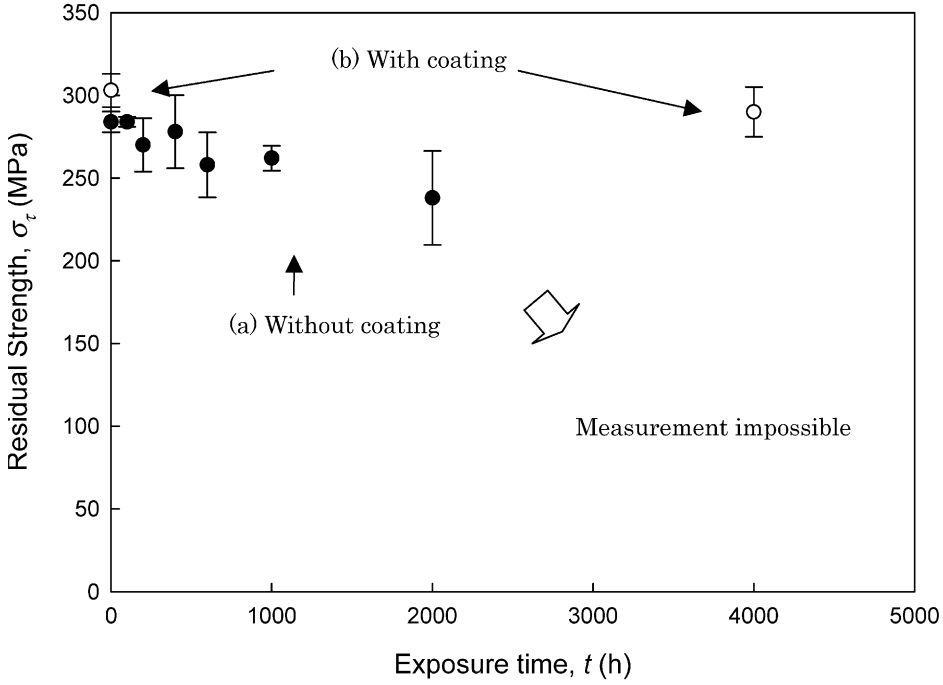

Fig. 6. Influence of oxidation at 1500 °C on the residual fracture strength of the samples measured with four-point flexural test (out-of-plane).

that the SiO_2 peaks appear upon oxidation of the sample with coating [Fig. 9(b)]. These SiO_2 peaks correspond to those of cristobalite. That is to say, the surface of the outer CVD-SiC layer is oxidized forming cristobalite and this oxidation behavior observed here is in good agreement with that of pure SiC. However, the samples without coating showed the reduced diffraction intensity of the SiO_2 peaks with an increment of heating time. Finally, no SiO_2 peaks but broad background could be observed corresponding to amorphous SiO_2 of the sample after 4000 h exposure [Fig. 9(a)]. These samples showed localized but heavy degradation with the color changing from the original dark purple-red color to white as mentioned earlier.

Then the questions arise, why the oxidized sample without coating shows reduced formation of cristobalite and why some of these samples are locally degraded. One possible explanation for these phenomena is that it was caused by the destruction of formed oxidation protective scale due to the bursting of the bubbles. The frequent bubble formation can be considered due to the high oxygen permeability through interstitial voids of SiO_2 scale containing Al ions. Namely, this composite forms an amorphous scale at 1500 °C composed of SiO_2 containing a few amounts of Al ions brought from the Si–C–Al–O fiber origin. This implies a high permeability of oxygen through the scale. Fig. 10(a) shows a structure model for the amorphous SiO_2 in top of the figure, and (b) that for the amorphous SiO_2 containing Al ions. The amorphous SiO_2 has a network structure of SiO_4^{4-} tetrahedra, and contains interstitial voids between tetrahedral through which O_2 molecules can diffuse. The oxidation process of SiC and of inside carbon is governed by the inward diffusion of O_2 molecules through the scale. As Al^{3+} ions occupy Si^{4+} sites, the interstitial voids increase and the oxidation rate becomes higher. The more Al ions content gives the more interstitial voids, resulting in the higher oxidation rate.

The amorphous SiO_2 scale with Al^{3+} ions on this composite does not crystallize during cooling after oxidation tests, because the solubility of Al_2O_3 is very small in β-cristobalite.[16] For the crystallization of SiO_2, Al^{3+} ions that occupy Si^{4+} site are required to diffuse away and precipitate as mullite. The process is so slow that crystallization of SiO_2 is suppressed.[17] Therefore, the SiO_2 scale that contains Al ions on this composite does not crystallize into cristobalite. Although amorphous SiO_2 has good scale adherence during cyclic oxidation, the residual stress in the excessively grown amorphous SiO_2 scale increases that will be resulting in spalling of the scale.

Although the samples coated with CVD-SiC were stable in this oxidation test, the cristobalite peaks observed by XRD suggest also inherent SiO_2 scale spalling problem due to the large volume change during the α–β phase transformation in cristobalite when it is cyclically heated. From the viewpoint of stability of SiO_2 scale, the tridymite is well known as displaying the lower volume change with alpha to beta phase transformation. In order to form tridymite in the oxidized

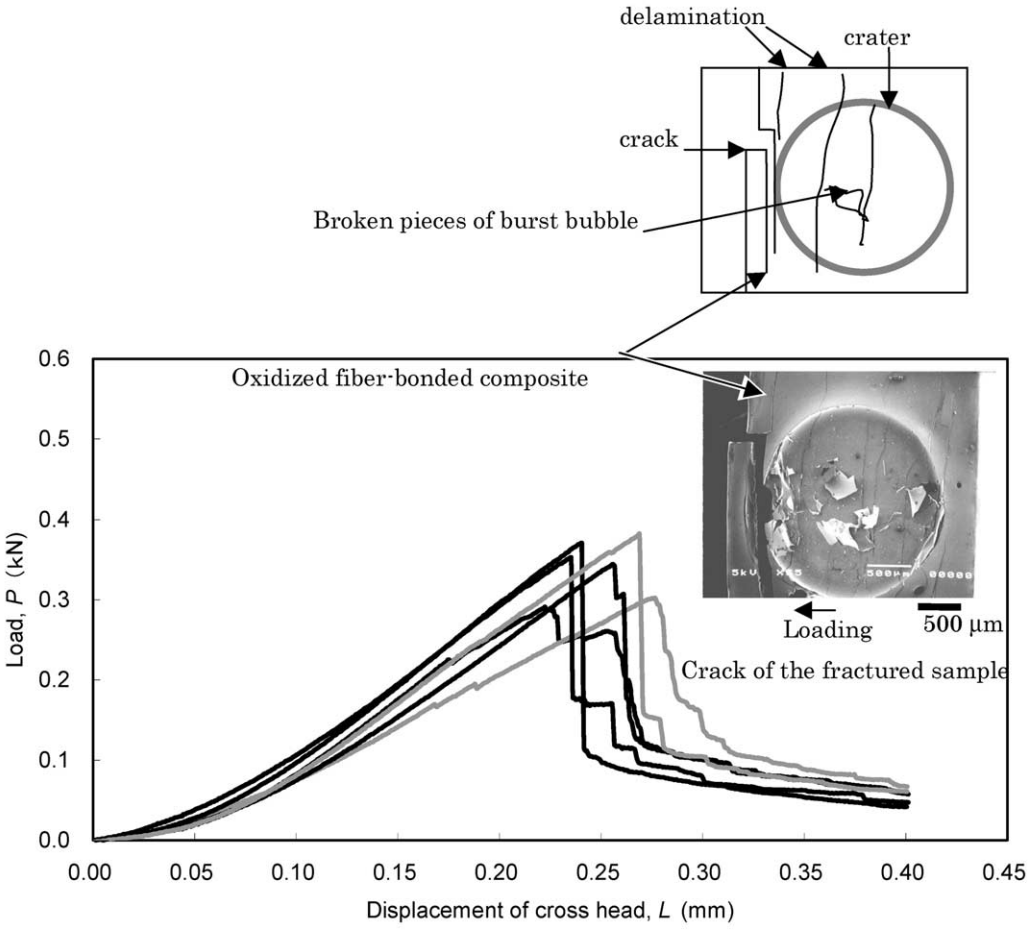

Fig. 7. Fracture behavior of the samples without coating after being oxidized for 2000 h. Burst bubble is formed on the surface of the sample by oxidation as it is apparent from the inserted SEM micrograph as a crater. Different curves show the dispersion of the measured value by four-point flexural test.

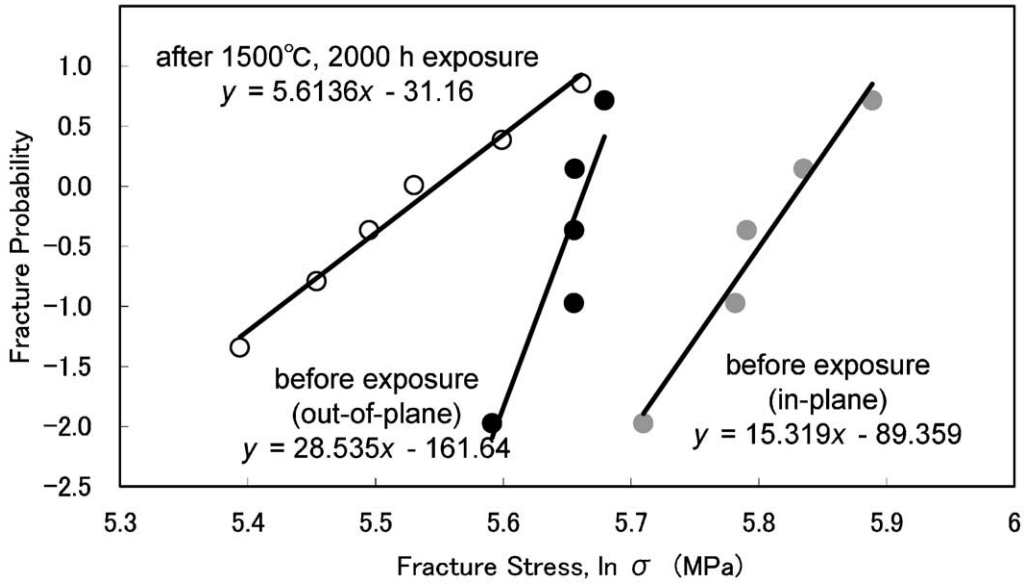

Fig. 8. Weibull plots of flexural fracture strength distribution of the samples before and after 2000 h oxidation. Filled circle and open circle indicate before and after oxidation, respectively.

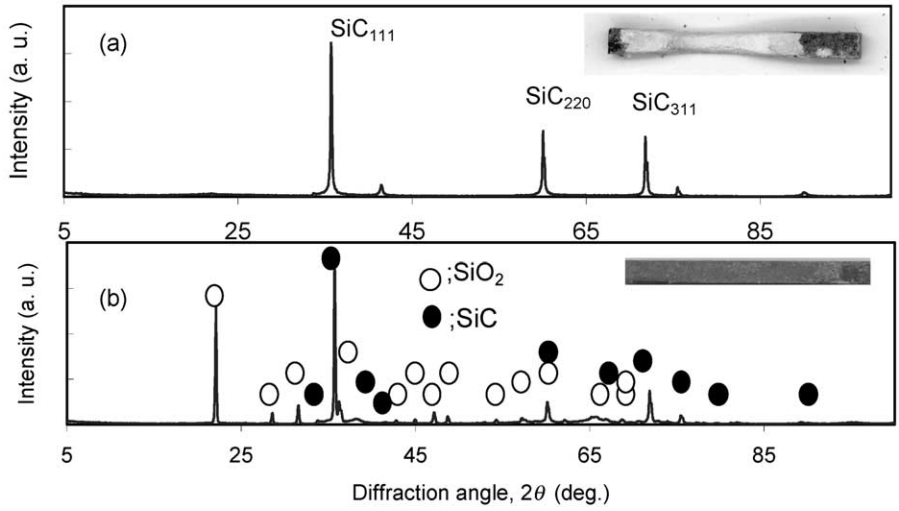

Fig. 9. XRD profiles (2θ scan, Cu-K_α rays) of the fiber composite sample after 4000 h oxidation: (a) without double layered SiC coating, (b) with double layered SiC coating.

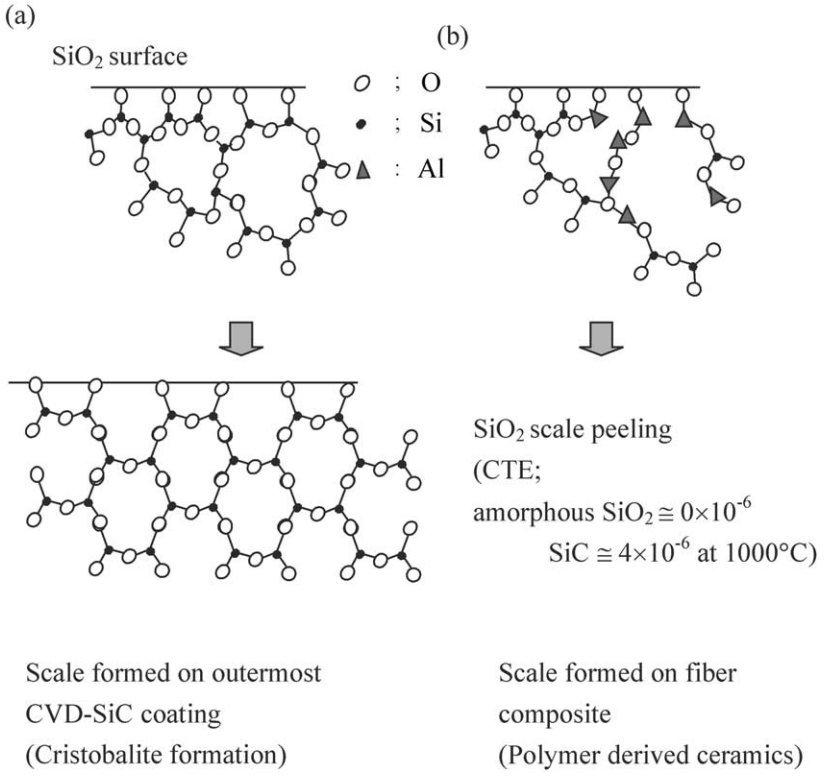

Fig. 10. Structure model for the cristobalite formation on double layered coated sample (a) and amorphous SiO_2 (b).

SiO_2 scale, addition of CaO etc. might be effective. However, the addition of a cation to the Si–O system will result in high oxygen permeability and a lowering of the viscosity of SiO_2 scale that will lead to excess formation of SiO_2. Therefore, further oxidation protective coating with some stable oxide on the CVD-SiC coating may be useful. This idea of the multi-coating system will be tested in near future.

4. Conclusion

The difference in oxidation behavior between Al containing fiber-bonded composite (Tyrannohex™) and CVD-SiC is the crystallinity of the formed SiO_2 scale. Large mass loss of Tyrannohex after 4000 h oxidation at 1500 °C in air is caused by destruction of oxidation protective scale due to bursting bubbles of amorphous

SiO_2 scale produced by the evolution of gaseous carbon oxides during heating. The high oxidation rate of Tyrannohex is brought by the high inward diffusion rate of O_2 molecules in the Al-doped SiO_2 scale. The inhibited crystallization of amorphous SiO_2 scale during long term oxidation tests can be explained by a slow diffusion rate of Al ions in the amorphous SiO_2 scale.

Although the samples coated with CVD-SiC were stable in this oxidation test, the cristobalite peaks observed by XRD suggest also an inherent problem of the SiO_2 scale spalling due to the large volume change during the α–β phase transformation during cyclic heating.

References

1. Yajima, S., Hayashi, J. and Omori, M., Synthesis of continuous SiC fibers with high tensile strength. *J. Am. Ceram. Soc.*, 1976, **59**, 324–327.
2. Bouillon, E., Langlais, F., Pailler, R., Naslain, R., Cruege, F., Huong, P. V., Sarthou, J. C., Delpuech, A., Laffon, C., Lagarde, P., Monthioux, M. and Oberlin, A., Conversion mechanisms of a polycarbosilane precursor into an SiC-based ceramic material. *J. Mater. Sci.*, 1991, **26**, 1333–1345.
3. Bill, J. and Aldinger, F., Precursor-derived covalent ceramics. *Adv. Mater.*, 1995, **7**(9), 775–787.
4. Laine, B. M. and Babonneau, F., Preceramic polymer routes to silicon carbide. *Chem. Mater.*, 1993, **5**, 260–279.
5. Sugimoto, T., Shimoo, T., Okamura, K. and Seguchi, T., Reaction mechanisms of silicon carbide fiber synthesis by heat treatment of polycarbosilane fibers cured by radiation. *J. Am. Ceram. Soc.*, 1995, **78**(7), 1849–1852.
6. Chollon, G., Czerniak, M., Pailler, R., Bourrat, X., Naslain, R., Pillot, J. P. and Cannet, R., A model SiC-based fibre with low oxygen content prepared from a polycarbosilane precursor. *J. Mater. Sci.*, 1997, **32**, 893–911.
7. Ishikawa, T., Kohtoku, Y., Kumagawa, K., Yamamura, T. and Nagasawa, T., High-strength alkali-resistant sintered SiC fibre stable to 2,200 °C. *Nature (London)*, 1998, **391**, 773–775.
8. Ishikawa, T., Kajii, S., Hisayuki, T. and Kohtoku, Y., SiC polycrystalline fiber and the fiber-bonded ceramic. In *Proceedings of the 6th Japan International SAMPE Symposium*, ed. T. Tanimoto and T. Mori, Tokyo, 1999, 1, pp. 253–256.
9. Heneger, C. H. Jr. and Jones, R. H., The effects of an aggressive environment on subcritical crack growth of a continuous-fiber ceramic composites. *Ceram. Eng. Sci. Proc.*, 1992, **13**(7–8), 411–419.
10. Filipuzzi, L., Camus, G., Naslain, R. and Thebault, J., Oxidation mechanisms and kinetics of 1D-SiC/C/SiC composite materials: I, an experimental approach. *J. Am. Ceram. Soc.*, 1994, **77**(2), 459–466.
11. Windisch, C. F. Jr., Henager, C. H. Jr., Springer, G. D. and Jones, R. H., Oxidation of the carbon interface in nicalon-fiber-reinforced silicon carbide composite. *J. Am. Ceram. Soc.*, 1997, **80**(3), 569–574.
12. Lara-Curzio, E., Stress-rupture of nicalon/SiC continuous fiber ceramic composites in air at 950 °C. *J. Am. Ceram. Soc.*, 1997, **80**(12), 3268–3272.
13. Morscher, G. N., Tensile stress rupture of SiC_f/SiC_m mini-composites with carbon and boron nitride interfaces at elevated temperatures in air. *J. Am. Ceram., Soc.*, 1997, **80**(8), 2029–2042.
14. Otsuka, A., Sakamoto, K. and Masumoto, H., A multi-layer CVD-SiC coating for oxidation protection of carbon/carbon composite. *Mater. Sci. Res. Int*, 1999, **5**(3), 163–168.
15. Otsuka, A., Matsumura, Y., Masumoto, H., Kitagawa, K. and Arai, N., Improvement in oxidation resistance of a C/C composite by using CVD-SiC coating with SiC fiber-composite layer. *TANSO 2000*, 2000, **194**, 254–260.
16. Frischat, G. H., Evidence for calcium and aluminum diffusion in SiO_2 glass. *J. Am. Ceram. Soc.*, 1969, **42**, 625.
17. Aramaki, S. and Roy, R., The mullite-corundum boundary in the systems $MgO–Al_2O_3–SiO_2$ and $CaO–Al_2O_3–SiO_2$. *J. Am. Ceram. Soc.*, 1959, **42**, 644–645.